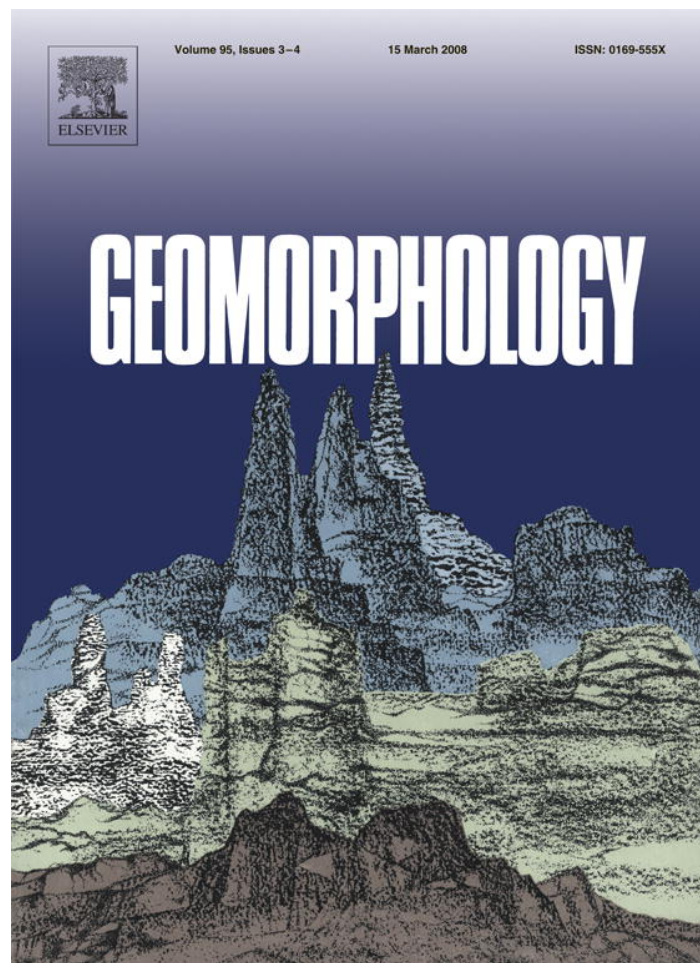


Provided for non-commercial research and education use.  
Not for reproduction, distribution or commercial use.



This article was published in an Elsevier journal. The attached copy is furnished to the author for non-commercial research and education use, including for instruction at the author's institution, sharing with colleagues and providing to institution administration.

Other uses, including reproduction and distribution, or selling or licensing copies, or posting to personal, institutional or third party websites are prohibited.

In most cases authors are permitted to post their version of the article (e.g. in Word or Tex form) to their personal website or institutional repository. Authors requiring further information regarding Elsevier's archiving and manuscript policies are encouraged to visit:

<http://www.elsevier.com/copyright>



## Post-wildfire erosion response in two geologic terrains in the western USA

John A. Moody<sup>a,\*</sup>, Deborah A. Martin<sup>a</sup>, Susan H. Cannon<sup>b</sup>

<sup>a</sup> U. S. Geological Survey, 3215 Marine Street, Suite E-127, Boulder, Colorado 80303, United States

<sup>b</sup> U. S. Geological Survey, Golden, Colorado, United States

Received 5 January 2007; received in revised form 21 May 2007; accepted 21 May 2007

Available online 8 June 2007

---

### Abstract

Volumes of eroded sediment after wildfires vary substantially throughout different geologic terrains across the western United States. These volumes are difficult to compare because they represent the response to rainstorms and runoff with different characteristics. However, by measuring the erosion response as the erodibility efficiency of water to detach and transport sediment on hillslopes and in channels, the erosion response from different geologic terrains can be compared. Specifically, the erodibility efficiency is the percentage of the total available stream power expended to detach, remobilize, or transport a mass of sediment. Erodibility efficiencies were calculated for the (i) initial detachment, and for the (ii) remobilization and transport of sediment on the hillslopes and in the channels after wildfire in two different geological terrains.

The initial detachment efficiencies for the main channel and tributary channel in the granitic terrain were  $10 \pm 9\%$  and  $5 \pm 4\%$  and were similar to those for the volcanic terrain, which were  $5 \pm 5\%$  and  $1 \pm 1\%$ . No initial detachment efficiency could be measured for the hillslopes in the granitic terrain because hillslope measurements were started after the first major rainstorm. The initial detachment efficiency in the volcanic terrain was  $1.3 \pm 0.41\%$ . The average remobilization and transport efficiencies associated with flash floods in the channels also were similar in the granitic ( $0.18 \pm 0.57\%$ ) and volcanic ( $0.11 \pm 0.41\%$ ) terrains. On the hillslope the remobilization and transport efficiency was greater in the volcanic terrain (2.4%) than in the granitic terrain (0.65%). However, this may reflect the reduced sediment availability after the first major rainstorm (30-min maximum rainfall intensity  $\sim 90 \text{ mm h}^{-1}$ ) in the granitic terrain, while easily erodible fine colluvium remained on the hillslope after the first rainstorm (30-min maximum rainfall intensity =  $7.2 \text{ mm h}^{-1}$ ) in the volcanic terrain. The erosion response in channels and on hillslopes of the granitic and volcanic terrains was similar when compared using erodibility efficiencies.

Published by Elsevier B.V.

*Keywords:* Wildfire; Erosion and deposition; Channels; Hillslope; Erodibility efficiency

---

### 1. Introduction

The erosion response after wildfire includes detachment, transport, and deposition of sediment particles by

water and gravity energy. Many post-wildfire erosion studies have focused on mountainous watersheds in a single geologic terrain. A wide variety of methods have been used to quantify erosion after wildfires under natural conditions (i.e., not using simulated rainfall) at different temporal and spatial scales. These methods can be grouped as (i) plot method (Daniel et al., 1943; DeBano and Conrad, 1976; Blong et al., 1982; Booker

---

\* Corresponding author.

E-mail addresses: [jamoody@usgs.gov](mailto:jamoody@usgs.gov) (J.A. Moody), [damarin@usgs.gov](mailto:damarin@usgs.gov) (D.A. Martin), [cannon@usgs.gov](mailto:cannon@usgs.gov) (S.H. Cannon).

et al., 1995; Scott et al., 1998; Moody and Martin, 2001a; Cannon et al., 2001a); (ii) silt fences (Robichaud et al., 2001; Benavides-Solorio and MacDonald, 2005); (iii) reservoir trapping method (Anderson, 1949; Rowe et al., 1954; Lavine et al., 2006); (iv) suspended-sediment method (Brown, 1972; Scott et al., 1998); and (v) the erosion-pin method (Doehring, 1968; Megahan and Moliter, 1975; White and Wells, 1984; Booker, 1998). Besides the different methodologies, the different spatial and temporal scales of these methods, and the different characteristics and magnitudes of the rainfall, hillslope runoff, and subsequent floods make comparisons of the erosion response (as mass or volume of sediment) between different terrains nearly impossible. However, land managers need to know how to make such comparisons so they can apply the erosion results from previously burned watersheds to newly burned watersheds.

The erodibility efficiency can be used to compare the erosion response for different hydrologic and geologic conditions. The efficiency is a measure of the percentage of water energy expended to do work in the form of detachment, remobilization, and transport of sediment. It is often calculated as the sediment mass transport rate normalized by the stream power and has been used in perennial and ephemeral streams (Yang, 1972; Bagnold, 1973; Wilson, 1999). This normalization will lead to meaningful efficiencies that are comparable, if the relation between sediment mass transport and stream power is linear. Linear relations appear to be associated with transport-limited systems (Reid and Laronne, 1995; Almedej and Diplas, 2005). For example, before a fire, a steep mountain perennial stream with an armored channel was a supply-limited system and had a non-linear relation (Moody and Martin, 2001a,b) similar to other perennial streams (Reid and Laronne, 1995). This changed to a nearly linear relation when sediment, eroded by flash floods after a wildfire, filled the channels and the system became transport-limited (Moody and Martin, 2001a,b; Moody, 2001). Other transport-limited systems, with steep channels and subjected to flash floods, have been shown by Reid and Laronne (1995) to have a linear relation between bedload transport rate and stream power.

Detachment, remobilization, and transport of soil or sediment particles are complex processes. These processes partly depend on the thermal and elastic properties inherited from the parent bedrock (Allison and Bristow, 1999), on the physical, chemical, and geometric properties of the soil (DeBano et al., 1977; Wiberg and Smith, 1987; Moody et al., 2005), and on the cohesive forces between these soil or sediment particles (Giovannini et al., 1988; Renard et al., 1997;

Gerits et al., 1990). Thus, the detachment, remobilization, and transport processes may vary between different geologic terrains and may affect the erodibility efficiency or erosion response. In this paper, we test the hypothesis that the erosion response after wildfire depends on the geologic terrain. We use the same method to quantify the runoff and the mass of eroded and transported sediment in two different, severely burned watersheds. One watershed is in granitic terrain and one is in volcanic terrain. We compute (i) the initial detachment efficiency, and (ii) the remobilization and transport efficiency for the channels and hillslopes in each geologic terrain and use these efficiencies to compare the erosion response.

## 2. Field setting

The two watersheds were similar in drainage area (Table 1). The granitic watershed (Spring Creek) was burned in 1996 by the Buffalo Creek Fire in the Front Range Mountains near Denver, CO, USA (Fig. 1) and is on the ~70-million-year old Pikes Peak granitic batholith (Moore, 1992). The volcanic watershed (Rendija Canyon) was burned in 2000 by the Cerro Grande Fire near Los Alamos, NM, USA (Fig. 1) and is on the flanks of the Jemez volcanic caldera, which erupted ~1 million years BP (Griggs and Hem, 1964; Kempton and Kelley, 2002).

Properties of the soils on the hillslopes and the sediment in the channel were different in these two geologic terrains. In the granitic terrain, the soils are classified as part of the Sphinx–Legault–Rock outcrop complex derived from gr $\ddot{u}$ s produced by weathering of the Pikes Peak granite. It has coarse texture and the average of samples from north- and south-facing hillslopes had a unimodal size distribution (Table 1, Fig. 2) with 10% silt and clay, 33% sand, and 57% gravel. In the volcanic terrain, the soils are derived from rhyodacite volcanic tuffs (Tschicoma Formation and Bandelier Tuffs) consisting of thick lava flows of latite and quartz latite (Griggs and Hem, 1964). This also has weathered into a type of gr $\ddot{u}$ s (D.E. Broxton, Los Alamos National Laboratory, personal communication, 2001) having a trimodal size distribution (Table 1, Fig. 2) with 24% silt and clay, 60% sand, and 16% gravel. The larger gravel and cobble-size volcanic sediments are more porous than the granitic sediments, had a lower dry density (Table 1), and absorbed an amount of water approximately equal to their dry weight.

Different tree densities in the two watersheds were observed to influence erosion patterns on hillslopes. Sparse tree density in the granitic terrain (Table 1) created long unobstructed hillslope segments with rills

Table 1  
Characteristics of the two watersheds

Characteristic	Spring Creek Colorado	Rendija Canyon New Mexico
Geological terrain	Granitic	Volcanic
Watershed area (ha)	2680	2480
Relief ratio	0.046	0.065
Channel slopes	0.03–0.33	0.04–0.39
Typical channel width (m)	8–50	5–10
Contributing area of main channels (ha)	2680	180 (north branch)
Contributing area of main channels (ha)	–	310 (south branch)
Contributing area of tributaries (ha)	3.7	24
Vegetation-hillslope	Ponderosa pine, Douglas-fir	Ponderosa pine
Vegetation-channel	Willow, narrowleaf cottonwood	Ponderosa pine
Vegetation density (stems ha <sup>-1</sup> )	400	3000
Fire & date	Buffalo Creek— 1996	Cerro Grande— 2000
Percent burned	79	78
Mean annual rainfall (mm)	420	610
Estimated mean annual discharge (m <sup>3</sup> s <sup>-1</sup> ) <sup>a</sup>	0.01	0.001
<i>Hillslope</i>		
Soil-median diameter (mm)	2.6–2.9	0.73
Soil-sorting (geometric standard deviation)	4.2–4.9	12.6
<i>Channels</i>		
Sediment-dry density (kg m <sup>-3</sup> )	2600	1700
Sediment-submerged density (kg m <sup>-3</sup> )	2600	2200
Median diameter of channel sediment (mm)	2.5	10

<sup>a</sup> Estimated from discharge at gage in Spring Creek for 2000; estimated by extrapolation of mean annual discharge per unit drainage area from Los Alamos Canyon, which is adjacent to Rendija Canyon (Shaull et al., 2000).

(Moody and Martin, 2001a,b). The tree density in the volcanic terrain was greater and this created more obstructions that curtailed long unobstructed rills. Differences in tree species also affected the post-fire hydrologic response of the channels. In the granitic terrain one month after the fire, a flood removed all the riparian vegetation (mostly willows, *Salix sp.* and cottonwood trees, *Populus sp.*), which reduced the vegetation drag (Smith, 2004) and increased the boundary shear stress available for detachment, remobilization, and transport of sediment. In the volcanic terrain, the channel had a dense population of ponderosa

pinus (*Pinus ponderosa*, diameters at breast height >0.2 m; Balice et al., 2000) spaced ~1–2 m apart in the channels. The trees were killed by the fire, but the trunks remained. These “stems” protruded through the flow in the channel and created drag (Smith, 2004), which reduced the boundary shear stress available for detachment, remobilization, and transport of sediment.

Both watersheds are in a semiarid climate with rainfall regimes characterized by short-duration, high-intensity convective rainfall. In the granitic terrain, the 30-min duration rainfall intensities are 32, 45, 54, 80, and 94 mm h<sup>-1</sup> for the 2-, 5-, 10-, 50-, and 100-year recurrence intervals (Miller et al., 1973). These are similar to the values of 34, 48, 58, 79, and 88 mm h<sup>-1</sup> in the volcanic terrain (Reneau et al., 2003). The mean annual rainfall (Table 1) is less over the granitic watershed than over the volcanic watershed, but the mean annual discharge is an order of magnitude greater in the granitic than in the volcanic watershed.

### 3. Methods

We selected research sites within the burned areas of each terrain that obviously had burned at high severity. Both terrains met the following descriptive characteristics for a high severity burn (Ryan and Noste, 1985; National Wildfire Coordinating Group, 1994): (i) a deep ash layer was present, (ii) all or most organic matter was consumed, (iii) essentially all plant parts in the duff layer were consumed, (iv) the entire canopies of twigs and small branches were completely consumed, (v) a few large branches remained but those were deeply charred, (vi) sound logs were deeply charred and rotten logs were completely consumed, and (vii) deep ground char was observed in scattered patches where logs or stumps produced prolonged intense heat that changed the color of the top layer of mineral soil. This selection of sites insured that the burn severity was similar enough that differences in erosion response were a result of differences in geology, rather than burn severity.

#### 3.1. Erosion response

The erosion response was measured as the erodibility efficiency. We calculated two efficiencies (i) the initial detachment efficiency and (ii) the remobilization and transport efficiency. They were calculated separately for the channels and for the hillslopes. We calculated the peak stream power, which is a measure of the peak energy per unit area per unit time and is a function of the peak water discharge, and measured the mass of eroded and deposited sediment.



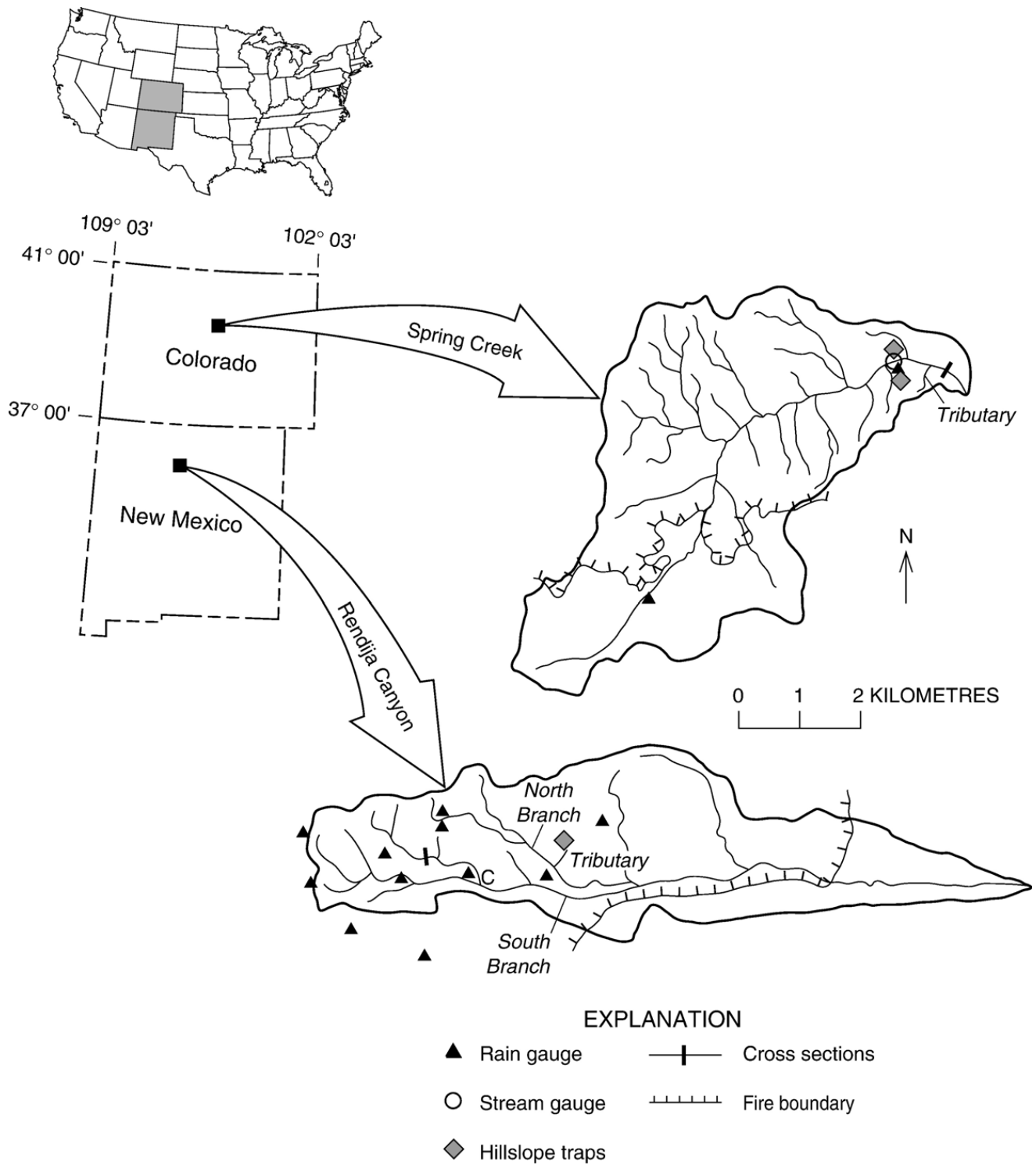


Fig. 1. Location of Spring Creek and Rendija Canyon watersheds and the fire boundaries. Some of the cross sections shown in Upper Rendija Canyon were used to calibrate the photogrammetry method. The cross sections below the stream gage in Spring Creek are not shown because they are too numerous (150 sections) to be shown at this scale.

### 3.2. Peak water discharge

Peak water discharge in channels was determined by indirect field methods for calculations of the initial detachment efficiencies and by an empirical relation

involving the rainfall intensity for calculation of the remobilization and transport efficiencies. The different methods were used because field measurement were obtained after the first flood associated with the initial detachment of sediment but field measurements could

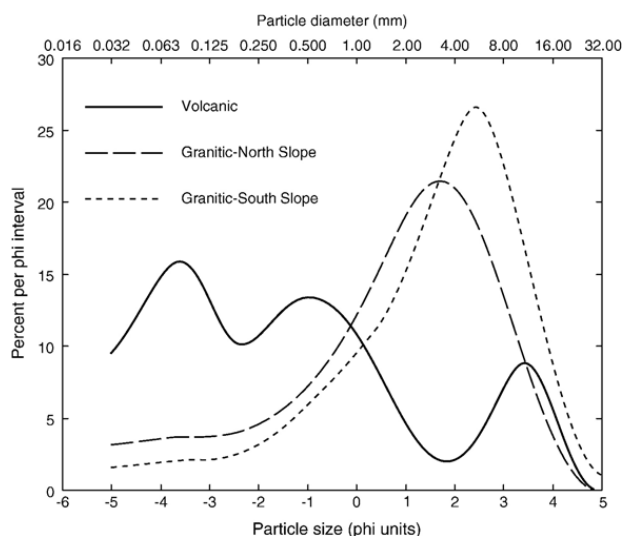


Fig. 2. Particle-size distribution of hillslope colluvium.

not logistically be made after each of the succeeding floods responsible for the remobilized and transported sediment.

Peak discharges for the initial detachment efficiency were calculated by using the indirect slope–area method (Rantz et al., 1982; Moody and Martin, 2001a) at multiple locations, the high water marks, and by assuming critical flow. For critical flow, the peak velocity,  $v^{\text{peak}}$ , is a function ( $v^{\text{peak}} = (gh^{\text{peak}})^{1/2}$ ) of only the peak water depth,  $h^{\text{peak}}$  and the acceleration of gravity,  $g$  ( $9.8 \text{ m s}^{-2}$ ). Thus, the peak discharge assuming critical flow,  $Q_{\text{peak}}^c$  ( $\text{m}^3 \text{ s}^{-1}$ ), is given by

$$Q_{\text{peak}}^c = v^{\text{peak}} a. \quad (1)$$

Critical flow has been shown by Jarrett (1987) and Grant (1997) to model flow conditions characterized by high-gradient streams with abundant sediment in mobile beds of sand and gravel. They also have argued for critical flow in mountainous streams characterized by high relative roughness where particle diameters of bed material are on the order of the flow depth. The roughness extracts energy from the mean flow in the

form of hydraulic jumps creating a hydraulic “brake” on flow accelerations especially in step-pool systems. Critical flow was used successful to model the discharge in Spring Creek in the burned granitic terrain (Moody and Martin, 2001a) and was assumed in the channels in the volcanic terrain, which had after the first flood, numerous burned tree stems, abundant sediment forming mobile beds, and large relative roughness in the form of debris and boulders that create a step-pool system.

The peak discharges, used to calculate a time series of remobilization and transport efficiencies at a cross section, were based on empirical relations between peak discharge,  $Q_{\text{peak}}^e$  ( $\text{m}^3 \text{ s}^{-1}$ ), and the maximum 30-min rainfall intensity,  $I_{30}$  ( $\text{mm h}^{-1}$ ). This relation had the form:

$$Q_{\text{peak}}^e = \beta (I_{30} - I_{30}^{\text{thres}}) A \quad (2)$$

where  $\beta$  ( $\text{m}^3 \text{ s}^{-1} \text{ km}^{-2} \text{ mm}^{-1} \text{ h}$ ) is a constant,  $I_{30}^{\text{thres}}$  is the rainfall intensity threshold for the initiation of runoff (Moody and Martin, 2001b; Moody et al., in press), and  $A$  is the drainage area upstream from the cross section. This drainage area was greater in the granitic terrain ( $26.80 \text{ km}^2$ ) than in the volcanic terrain ( $1.26 \text{ km}^2$ ) so that the constant  $\beta A$  for the granitic terrain was greater than the constant for volcanic terrain (Table 2). Only one of the total 20 measurements in the granitic terrain was based on the empirical equation for 1999 with the lowest  $R^2$ -value. The rainfall intensity thresholds appear to increase with time (Table 2), but the number of samples per year was insufficient to support this statistically. However, separate equations were used for each time period because  $b$  was substantially different for some time periods.

### 3.3. Rainfall intensity

Tipping-bucket recording rain gages were used to measure rainfall intensity within each burned watershed. These rain gages had a 0.152-m diameter opening (Onset, model RG-1 and RG-2), were calibrated in the laboratory, and recorded the time of each tip equal to

Table 2  
Parameters used to calculate peak discharge in the equation  $Q_{\text{peak}}^e = \beta(I_{30} - I_{30}^{\text{thres}})A$

Terrain	Time period	$\beta$		$A$ ( $\text{km}^2$ )	$\beta A$ ( $\text{m}^3 \text{ s}^{-1}/\text{mm h}^{-1}$ )	$I_{30}^{\text{thres}}$ ( $\text{mm h}^{-1}$ )	$R^2$
		( $\text{m}^3 \text{ s}^{-1}/\text{km}^2/\text{mm h}^{-1}$ )	(Non-dimensional form)				
Granitic	1996–1997	0.21	0.75	26.8	5.6	4.1	0.80
	1998	0.088	0.32	26.8	2.4	4.3	0.88
	1999	0.0032	0.012	26.8	0.086	3.1	0.14
	2000	0.0024	0.009	26.8	0.064	7.3	0.92
Volcanic	2000–2001	0.14	0.50	1.26	0.18	7.6	0.73
	2002–2003	0.12	0.43	1.26	0.15	11.1	0.52

0.254 mm of rain. These data were used to evaluate the hillslope erosion trap data, to determine the duration of time that the rainfall intensity was greater than the threshold necessary to initiate overland flow, and to calculate peak discharges using Eq. (2).

### 3.4. Measurements of the mass of eroded and deposited sediment

#### 3.4.1. Channels

Initially, during the first flood, sediment was eroded from low order channels and deposited in higher order channels, but later floods eroded and deposited sediment in all channels with various magnitudes. We assumed (based on field observations after the first flood) that the volume of sediment eroded from the main channel was smaller than the volume of sediment deposited. Thus, for calculating the initial detachment efficiency in the main channels, the deposited sediment was the sum of the change in cross-sectional area (at multiple, uniformly spaced cross sections) times the distance between the cross sections.

In the granitic terrain, the volume of deposited sediment after the first flood was determined by using photogrammetric methods. We used aerial photographs (1:12,000 scale) taken before (June 1996) and after (August 1996) the first flood and made measurement at cross sections spaced 60 m apart. This method was verified later using aerial photographs and cross sections surveyed on the ground. For tributaries, the top width, bottom width, depth, and side slope of the eroded channels were measured at each cross section spaced 5 m apart.

In the volcanic terrain, the volume of deposited sediment after the first flood also was determined by using aerial photographs (1:6000 scale). The cross sections were measured photogrammetrically using photographs taken before (June 2000) and after (July 2000) the first flood and were spaced 100 m apart. Cross sections were surveyed on the ground and used to verify the photogrammetric method. Both methods were used for the tributaries. Cross sections were spaced 4 and 40 m apart for the ground surveys and 100 m apart on aerial photographs (1:6000 scale).

A time series of remobilization and transport efficiencies was computed at one of the cross sections on a main channel in each terrain. The cross-sectional area was calculated from bed surface elevations, which were measured by (i) ground surveys using an automatic level and metric tape or (ii) photogrammetric analysis of aerial photographs. The sediment volume was equal to the net change in cross-sectional area times a unit length (1 m) of channel length. These volumes were converted to equivalent mass by multiplying by the average bulk

density based on multiple field samples. The cross-section was surveyed 20 times in the granitic terrain (1996 through 2001) and 5 times in the volcanic terrain (2000 through 2003). Both cross sections had similar geometry and geomorphology. The width was about 45 m, which included a small step in the floodplain of ~1–2 m above the stream bed on the left bank, and both cross sections were near the middle of the study reach.

#### 3.4.2. Hillslopes

Field based measurements of hillslope erosion and deposition were started 1 year after the fire in the granitic terrain and two weeks after the fire in the volcanic terrain (Fig. 3). Thus, the initial detachment efficiency was only calculated for the volcanic terrain, but remobilization the transport efficiencies were calculated for both terrains.

In the granitic terrain, water and sediment were collected in 1-m-wide hillslope traps from a bounded area. Details of these hillslope traps are described by Gerlach (1967) and Moody and Martin (2001a). The bounded area ranged from 5–10 m<sup>2</sup>, was about 5 m long, and enclosed some existing rills on 30° slopes (Martin and Moody, 2001). Runoff and sediment were stored in three collecting containers (~45 L capacity) and the volumes of water and mass of sediment in the containers were measured from 1997 to 2001 (Fig. 3). Four hillslope traps on a north-facing hillslope collected water and sediment volumes during 9 rainstorms (water-collecting containers overflowed during four storms), and four hillslope traps on a south-facing hillslope collected water and sediment volumes during 13 rainstorms. The amount of runoff and eroded sediment for each hillslope was the mean of the four traps. This mean was used to calculate an efficiency for each hillslopes and for each rainstorm. The final efficiency was the average of all rainstorms.

In the volcanic terrain, water and sediment were collected in similar hillslope traps but with an unbounded area. The traps were on 25–30° slopes, on a southeast-facing hillslope, at a distance of 108–217 m down from the drainage divide, and had no existing rills above them (Cannon et al., 2001b). These traps stored water and sediment in three collecting container (~45 L capacity), which were measured from June through October 2000 (Cannon et al., 2001b). The final efficiency for each rainstorm was the mean value of 4 to 9 hillslope traps. We only used data for rainstorms >30 min, but the single storage containers could possibly overflow undetected, if the total rainfall was >15 mm and the maximum 30-min rainfall intensity was >15 mm h<sup>-1</sup>. Therefore, any data that met these conditions were not used. The initial detachment efficiency was based on the first rainstorm

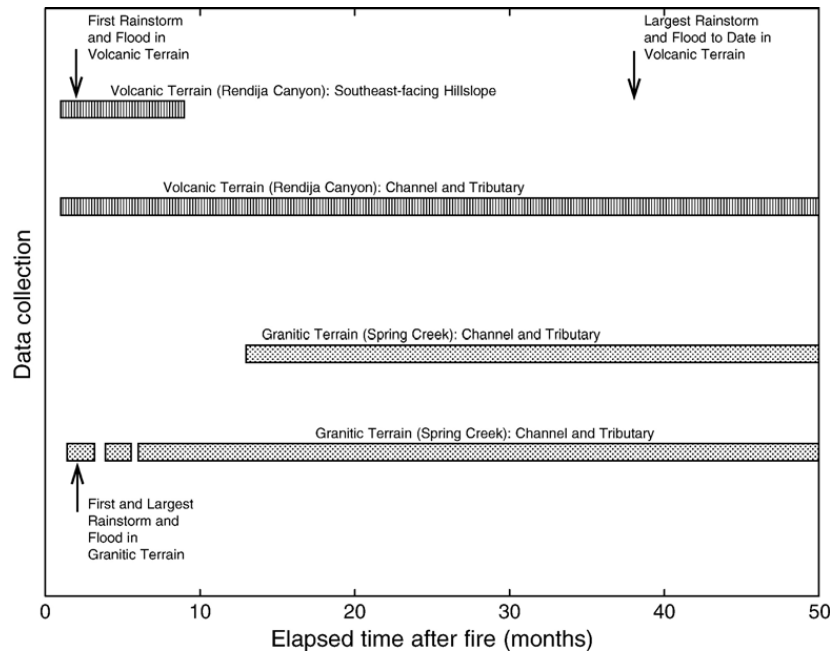


Fig. 3. Time line showing the data collection periods and the times of the first and largest rainstorms and floods in the watersheds of the two geologic terrains.

(nine replicate samples) and the remobilization and transport efficiency was based on 4 rainstorms.

### 3.5. Initial detachment efficiency

The channel bank sediment and hillslope colluvium detached during the first flood after the fire probably had some degree of cohesion. The cohesion developed during the period following deposition well before the fire burned in 2000. We assumed that the stream power to detach this cohesive material from channel banks or from hillslopes was much greater than the stream power required to transport it. Stream power can gradually detach particles from a cohesive channel bank or soil matrix or it can suddenly detach large volumes of sediment particles by such processes as head cut erosion (Bennett and Casali, 2001; Cannon et al., 2003) and by bank failures (Simon et al., 1999; Darby et al., 2002). Later, after the flood waters have receded, excess pore pressure in the channel banks can cause sudden detachment of large volumes of sediment (Simon and Collison, 2001). Based on field observations after the first flood, the sediment deposited in the channel was non-cohesive. Thus, the stream power associated with later floods was assumed to primarily remobilize and transport this non-cohesive sediment.

#### 3.5.1. Channels

The erodibility efficiency is the ratio of the available peak stream power and the fraction of that power (rate of

work) used to detach or transport sediment. The available peak stream power per unit area of channel bed,  $\omega_c$  ( $J m^{-2} s^{-1}$ ), is given by

$$\omega_c = \frac{\rho_w g Q_{peak}^c S}{B} \quad (3)$$

where  $\rho_w$  is the density of water =  $1000 \text{ kg m}^{-3}$ ,  $S$  is the bed slope of the channel, and  $B$  (m) is the channel width. This is the same as the overall transport efficiency for bedload used by Bagnold (1973). The fraction of this power or work,  $W_c$  ( $J m^{-2} s^{-1}$ ) that detaches sediment during the time interval,  $\Delta T$  (s), equals the submerged weight (mass  $\cdot g$ ) removal rate per unit width of channel,  $w_s$  ( $J m^{-2} s^{-1}$ ) multiplied by  $\tan \alpha$ . The angle  $\alpha$  is essentially the angle of internal friction of material being detached, is analogous to the sliding friction of a solid on a plane, and was shown by Bagnold (1973) to be  $\sim 32^\circ$  for most particles sizes. Thus:

$$W_c = w_s \tan \alpha = \frac{(\rho_s - \rho_w) g \rho_b V_s}{B \rho_s \Delta T} \tan \alpha \quad (4)$$

where  $\rho_s$  ( $kg m^{-3}$ ) is the sediment particle density,  $\rho_b$  ( $kg m^{-3}$ ) is the sediment bulk density, and  $V_s$  ( $m^3$ ) is the volume of sediment transported and deposited after the initial flood. Sediment is detached only when water discharge,  $Q$  ( $m^3 s^{-1}$ ), is  $> Q_{crit}$ , the critical discharge for sediment detachment. We have assumed that the critical discharge,  $Q_{crit}$ , for detachment was negligible compared to the peak discharge,  $Q_{peak}^c$ , during the initial



detachment. This assumption is based on the fact that the critical shear stress ( $1\text{--}3 \text{ N m}^{-2}$ ) required to detach unburned and burned cohesive forest soils on hillslopes (Moody et al., 2005) was much less than the estimated shear stress ( $400\text{--}800 \text{ N m}^{-2}$ ) associated with the peak discharge of the first flood ( $510 \text{ m}^3 \text{ s}^{-1}$ ) in the granitic terrain (water depth  $1\text{--}2 \text{ m}$ ). Thus, the time interval,  $\Delta T$ , can be considered equal to the duration of the flood,  $T$ . The initial detachment efficiency for channels,  $e_c$ , is

$$e_c = \frac{W_c}{\omega_c} * 100 \text{ for } Q_{\text{peak}}^c > Q_{\text{crit}} \quad (5)$$

which is independent of the channel width,  $B$ .

In the granitic terrain, the initial sediment was detached and trapped in an expanding reach near the mouth of Spring Creek. The reach was  $1500 \text{ m}$  long and the width was  $10 \text{ m}$  at the upstream end and widened to  $45 \text{ m}$  at the mouth (Moody, 2001). A small fraction of the sediment was deposited beyond the mouth and dammed the South Platte River. Part of this volume was eroded by the river in a few days. The eroded volume was measured by interpolating between the remaining sediment deposits on both sides of the South Platte River, and was included in the calculation of the initial detachment efficiency.

In the volcanic terrain, the initial sediment was detached from multiple headwater tributaries and deposited above the confluence of the two main channels (South and North Branch of upper Rendija Canyon; point marked “C” in Fig. 1). Separate efficiencies were calculated for the deposited volume in a  $1300\text{-m}$  reach on the South Branch and in a  $1100\text{-m}$  reach on the North Branch, and then averaged to determine the final initial detachment efficiency.

### 3.5.2. Hillslope

The hillslope stream power,  $\omega_h$ , was computed similar to Eq. (3), but the mean discharge was used instead of the peak discharge. There were no time series measurements of water depth at the entrance to the trap and so the peak discharge was unknown. The mean discharge per unit width of hillslope (with slope,  $S_h$ ) was measured by dividing the collected water volume,  $V_w$ , by the duration of the rainstorm,  $\Delta t$ , and the width,  $b$ , of the hillslope trap:

$$\omega_h = \frac{\rho_w g V_w S_h}{b \Delta t} \quad (6)$$

The duration was not necessarily continuous and was the sum of time intervals when the rainfall intensity was greater than the threshold necessary to initiate overland flow. Unpublished field observations indicate that this

threshold is similar to  $I_{30}^{\text{thres}}$  ( $\text{mm h}^{-1}$ ). The fraction of power or work,  $W_h$  ( $\text{J m}^{-2} \text{ s}^{-1}$ ), used during the same time interval,  $\Delta t$ , was

$$W_h = \frac{\left(\frac{\rho_s - \rho_w}{\rho_s}\right) Mg \tan \alpha}{b \Delta t} \quad (7)$$

where  $M$  (kg) is the mass of sediment collected in the trap. The initial detachment efficiency for hillslopes was computed as:

$$e_h = \frac{W_h}{\omega_h} * 100. \quad (8)$$

This efficiency is independent of the trap width. It is also independent of the duration of time when the rainfall is greater than the threshold because the hillslope colluvium is assumed to be transported during the same time,  $\Delta t$ , as the overland flow.

## 3.6. Remobilization and transport efficiency

### 3.6.1. Channel

The time series of remobilization and transport efficiencies at a channel cross section were calculated using a similar method as the initial detachment efficiency. Measurements at multiple cross sections ( $150$  cross sections spaced  $10 \text{ m}$  apart) in 1997 in the granitic terrain had similar patterns of scour and fill and the number of cross sections was reduced in subsequent years. (Moody and Martin, 2001a,b; Moody, 2001). Similar patterns were measured and observed in the volcanic terrain. Therefore, we feel the efficiencies calculated at one cross section were representative of the main channel. The total mass was equal to the sum of the net cross-sectional area of erosion and the net cross-sectional area of deposition times the bulk density and the unit stream length. This total mass was assumed to be proportional to the total work done to remobilize and transport sediment per unit area of channel and the peak discharge,  $Q_{\text{peak}}^c$ , was used in Eq. (3) instead  $Q_{\text{peak}}^c$  for the reasons given in Section 3.1.

### 3.6.2. Hillslope

Remobilization and transport efficiencies for hillslopes were calculated for each sample of water and sediment collected from the hillslope traps. Samples were not collected after each storm, but in most cases the data represent a dominant storm plus one to two smaller storms. Calculations differed from those for remobilization and transport in channels because the mass of sediment collected from the traps was measured directly and no conversion from volume to mass was required.

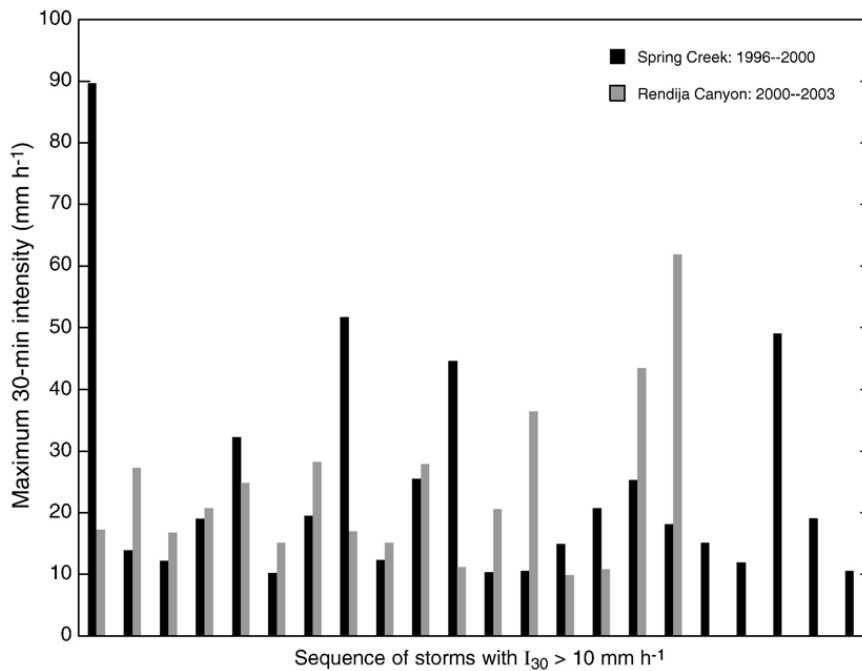


Fig. 4. Magnitude of a sequence of storms (only those with maximum 30-min rainfall intensity,  $I_{30} > 10 \text{ mm h}^{-1}$ ) in the granitic terrain (Spring Creek) and volcanic terrain (Rendija Canyon). The time interval between storms is different for each pair of storms and for each watershed.

Hillslope measurements in the granitic terrain represent the mean remobilization and transport efficiency of sediment for 22 samples collected from north-facing ( $n=9$ ) and south-facing ( $n=13$ ) hillslopes over 2 years (Moody and Martin, 2001a). Hillslope measurements in the volcanic terrain represent the mean remobilization and transport efficiency of four storms during the summer of 2000 after the first storm on 9 July 2000.

## 4. Results

### 4.1. Rainstorms

The first storm in the granitic terrain occurred 2 months after the wildfire and had the most intense rainfall (maximum  $I_{30} \sim 90 \text{ mm h}^{-1}$ ) of all the storms (Fig. 4). This intensity had about a 100-year rainfall

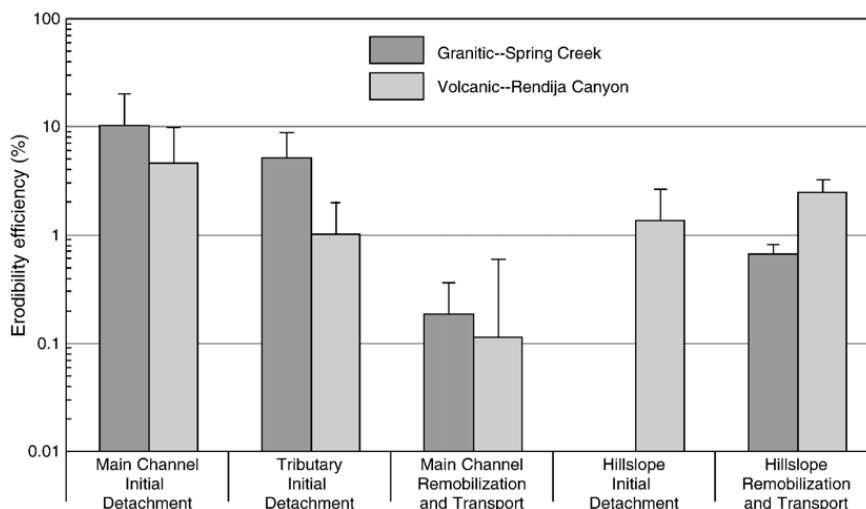


Fig. 5. Erodibility efficiencies measured after wildfire in the main and tributary channels, and on hillslopes in granitic and volcanic terrain. The main channel remobilization and transport efficiencies are those for periods with flash floods only (see Fig. 6). The bars indicate the estimate of the uncertainty in the calculation of each erodibility efficiency.

recurrence interval (Miller et al., 1973). In contrast, the first storm in the volcanic terrain was 1 month after the wildfire but was one of the smallest storms (maximum  $I_{30} \sim 17 \text{ mm h}^{-1}$ ), with a rainfall recurrence interval of slightly less than 1-year (Reneau et al., 2003). The most intense storm (maximum  $I_{30} \sim 62 \text{ mm h}^{-1}$ ) in the volcanic terrain was 3 years after the fire, and this had about a 25- to 50-year recurrence interval (Reneau et al., 2003).

#### 4.2. Erodibility efficiencies

The initial detachment efficiency for the main channel in the granitic terrain was 10% and in the volcanic terrain it was 5% (Fig. 5). Although the efficiency for the granitic terrain is larger the uncertainty of the values was greater in the granitic terrain than in the volcanic terrain (Table 3). This is in part due to averaging two estimates

in the volcanic terrain and the smaller absolute magnitude of the efficiency. The efficiencies in the tributary channels were less than in the main channel in both terrains. Again, the initial detachment efficiency in the granitic terrain (5%) was not significantly greater than in the volcanic terrain (4%).

The average initial detachment efficiency on the volcanic hillslopes was 1.3% (Fig. 5) from the first rainstorm on 9 July 2000. The coefficient of variance of the efficiencies for the nine traps was relatively high (1.6), which was influenced by one trap with an efficiency of 4.2%.

#### 4.3. Remobilization and transport efficiency

The average remobilization and transport efficiencies in the main channels of both terrains were about one order of magnitude less than initial detachment

Table 3  
Summary of erodibility efficiencies

	<i>N</i>	<i>B</i> (m)	$V_s/\Delta T$ ( $\text{m}^3 \text{ s}^{-1}$ )	$(\rho_s - \rho_w)/\rho_s$	$\rho_b$ ( $\text{kg m}^{-3}$ )	$\Delta T$ (h)	$q_s$ ( $\text{J m}^{-2} \text{ s}^{-1}$ )	$Q_{\text{peak}}$ ( $\text{m}^3 \text{ s}^{-1}$ )	<i>S</i>	$\omega_c$ ( $\text{J m}^{-2} \text{ s}^{-1}$ )	<i>e</i> (%)	$\Delta e$ (%)
<i>Channel initial detachment</i>												
<i>Granitic-Spring Creek</i>												
Main channel	1	8	3.0	0.62	1700	2	3909	510	0.04	24,990	10	±9
Tributary	1	6	0.08	0.62	1700	1	129	4.5	0.22	1617	5	±4
<i>Volcanic-Rendija Canyon</i>												
North branch	1	4	0.86	0.41	1000	1	859	26	0.10	6370	8	±6
South branch	1	4	0.11	0.41	1000	1	112	30	0.10	7350	1	±4
Tributary	1	2	0.056	0.41	1000	1	112	6.6	0.24	7762	1	±1
<i>Channel remobilization and transport</i>												
<i>Granitic-Spring Creek</i>												
Flash floods	10	45	<i>0.004167</i>	0.62	1700	1.2	<i>0.96</i>	<i>120</i>	0.04	<i>1045</i>	0.18	±0.57
Steady flow	10	45	<i>4.31E-07</i>	0.62	1700	3326	<i>0.0001</i>	<i>0.10</i>	0.04	<i>0.87</i>	0.007	±0.001
<i>Volcanic-Rendija Canyon</i>												
Flash floods	5	18	<i>0.00094</i>	0.41	1000	1	0.36	5.66	0.10	308	0.11	±0.41
	<i>N</i>	<i>b</i> (m)	<i>M/b</i> ( $\text{kg m}^{-1}$ )	$(\rho_s - \rho_w)/\rho_s$	$\rho_b$ ( $\text{kg m}^{-3}$ )	$\Delta T$ (h)	$q_s$ ( $\text{J m}^{-2} \text{ s}^{-1}$ )	$V_w/\Delta t$ ( $\text{m}^3 \text{ s}^{-1}$ )	<i>S<sub>h</sub></i>	$\omega_c$ ( $\text{J m}^{-2} \text{ s}^{-1}$ )	<i>e</i> (%)	$\Delta e$ (%)
<i>Hillslope initial detachment</i>												
<i>Volcanic-Rendija Canyon</i>												
South	1	1	<i>0.041</i>	0.41	na	0.50	<i>0.000091</i>	<i>0.0000018</i>	0.5	<i>0.0089</i>	1.3	±0.41
<i>Hillslope remobilization and transport</i>												
<i>Granitic-Spring Creek</i>												
North and South	22	1	<i>0.0701</i>	0.62	na	1.35	<i>0.00012</i>	<i>0.0000035</i>	0.5	<i>0.017</i>	0.65	±0.11
<i>Volcanic-Rendija Canyon</i>												
South	4	1	<i>0.26</i>	0.41	na	0.71	<i>0.00036</i>	<i>0.0000061</i>	0.5	<i>0.030</i>	2.4	±0.74

*N*, number of samples; *B*, channel width; *b*, plot width;  $V_s$ , volume of transported and deposited sediment;  $\rho_s$ , particle sediment density;  $\rho_w$ , water density =  $1000 \text{ kg m}^{-3}$ ;  $\rho_b$ , bulk density of deposited sediment;  $\Delta T$ , duration of flood;  $Q_{\text{peak}}$ , peak water discharge; *S*, slope of the channel or hillslope;  $\omega_c$ , stream power per unit area; *e*, erodibility efficiency for channel, tributary or hillslope;  $\tan\alpha$  is set equal to 0.63;  $\Delta e$ , estimate of the uncertainty of the erodibility efficiency; values shown in italics are the average of *N* measurements.

efficiency. The efficiencies were calculated for flash floods (10 in the granitic terrain and 5 in the volcanic terrain) and for the time periods of base flow between flash floods (Table 3, Fig. 6). The efficiency associated with flash floods in the granitic terrain (0.18%) was only slightly greater than the efficiency in the volcanic terrain (0.11%). Between flash floods, the granitic channel had some base flows with an efficiency of 0.007%. No water flowed in the volcanic channel between flash floods and thus no efficiencies were calculated.

The average remobilization and transport efficiency was substantially less on the granitic hillslopes (0.65%) than on the volcanic hillslope (2.4%). For the granitic terrain, the efficiency was the average of the efficiencies associated with 22 rainstorms on the north-(0.78%) and on the south-(0.55%) facing hillslopes. This relatively large sample number may be partly responsible to the

lower absolute uncertainty of  $\pm 0.11\%$ . The efficiency in the volcanic terrain was based on a sample of 4 rainstorms and had a larger uncertainty ( $\pm 0.74\%$ ). The relatively high uncertainty was partially caused by the relatively high efficiency (8%) associated with a single storm on 9 August 2000.

## 5. Discussion

### 5.1. The effects of rainstorm sequence

The sequence of rainstorms and subsequent floods has been shown to affect the geomorphic impact of wildfire (Germanoski et al., 2002). This was also true for these two geologic terrains. The most intense storm over the granitic terrain was the first storm. If it had been much later, following vegetation regrowth and the removal of some of the available sediment by relatively smaller storms, then the erosion response probably would have been much less. In contrast, the most intense storm in the volcanic terrain occurred 3 years after the wildfire. During the 3 years substantial regrowth of vegetation throughout the burned watershed was observed using color aerial photographs taken in 2000, 2001, and in 2002 and in the areas visited on the ground to service equipment. This regrowth attenuated the runoff response (Moody et al., *in press*) and the associated erosion response. Had this most intense storm been the first storm after the wildfire then the relative magnitude of the erosion response associated with this storm would have probably been greater than the magnitude after 3 years.

### 5.2. Initial detachment efficiency

The initial detachment efficiencies in the main channels are probably minimal estimates because (i) the peak discharge,  $Q_{\text{peak}}^c$ , in Eq. (5) minimizes the efficiency relative to the time-averaged discharge (which is  $< Q_{\text{peak}}^c$  but was not measured) and (ii) the duration,  $\Delta T$ , is probably a maximum estimate of the time for detachment. The detachment efficiencies for the main channels were based on measurements of deposition, which includes additional energy for transport, while those in the tributary were based solely on measurements of erosion or detachment. Thus, the detachment efficiencies for the main channels may be greater than those reported in Table 3.

It is interesting to compare the actual volumes used to calculate the initial detachment efficiencies in the tributaries because eroded volumes are occasionally published in the literature. In the granitic tributary, the average measured erosion was  $1.2 \text{ m}^3 \text{ m}^{-1}$ , and in the

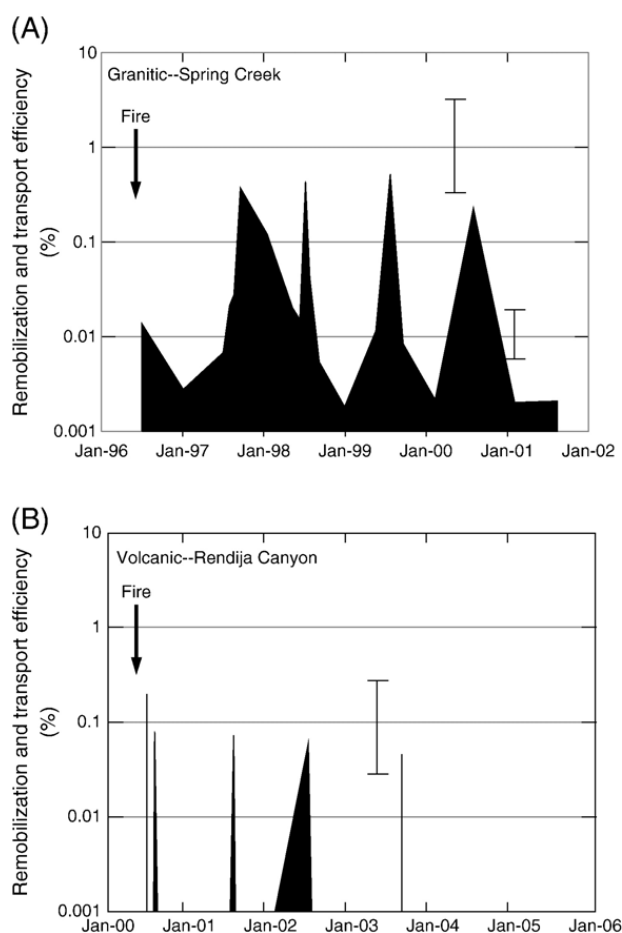


Fig. 6. Remobilization and transport efficiency calculated for the main channel: (A) Cross-section 341 in the granitic terrain from 2 June 1996–97 September 2003, and (B) Cross-section 11 in the volcanic terrain from 28 June 2000–5 October 2003. The bars indicate the estimate of the uncertainty in the calculation of the efficiency. The upper bar in Fig. 5A corresponds to flash floods and the lower bar is an estimate for the intervening remobilization and transport during steady flow.



volcanic tributary it was  $0.4 \text{ m}^3 \text{ m}^{-1}$ . These measurements are similar to other post-fire measurements in other terrains. For example,  $0.3\text{--}9 \text{ m}^3 \text{ m}^{-1}$  was measured in various terrains in California, Colorado, and Utah (Santi et al., *in press*);  $0.45 \text{ m}^3 \text{ m}^{-1}$  was measured in sandstone terrain in Arizona (Rich, 1962);  $0.44 \text{ m}^3 \text{ m}^{-1}$  in granitic terrain in Arizona (Laird and Harvey, 1986); and  $2.0 \text{ m}^3 \text{ m}^{-1}$  in marine sandstones and shales terrain of southern California (Florsheim et al., 1991). This relatively narrow range of volumes per meter of channel also indicates, like the efficiencies in this paper, little difference across geologic terrains.

The relatively high initial detachment efficiencies ( $>1\%$ ) in the main channel may be dominated by short timescale erosion processes. Efficiencies for many perennial streams are usually substantially  $<1\%$  (Reid and Laronne, 1995; Almedeij and Diplas, 2005). Short timescale erosion processes like head cutting (Bennett and Casali, 2001) or bank failure (Simon et al., 1999; Darby et al., 2002) involve undercutting and sudden collapse of channel bed or banks. In general, we have observed many bank failures and headcuts in the main channel and tributary channels of both terrains, which created step-pool topography. In some cases this topography in the main channel was either eroded or covered by sediment during some floods and uncovered by later floods. However, it was persistent in low order tributary channels. We assume that bank failure and head cut erosion are more efficient and thus they will, when present, substantially increase the initial detachment erodibility efficiency.

### 5.3. Remobilization and transport efficiency

#### 5.3.1. Channels

The remobilization and transport of sediment in the main channel and in tributary channels after the wildfires was episodic. Flow in channels in both terrains was observed to be ephemeral with shorter periods ( $\sim$  day to week) of no surface flow in the granitic terrain than in the volcanic terrain ( $\sim$  weeks). Two sediment transport processes were common in the granitic terrain. Sediment transport by flash floods was typically unsteady flow, with times scales of a few hours. Transport by base flow ( $\sim$  mean annual discharge =  $0.01 \text{ m}^3 \text{ s}^{-1}$ ; Table 1) was typically steady flow over time scales of days to months and was of sufficient discharge to appear as surface flow in most of the channel (Moody, 2001). Remobilization and transport efficiencies for individual flash floods were relatively high and ranged from  $0.021\text{--}0.52\%$ . These efficiencies are not unusual as flash floods in other ephemeral channels fall within a relatively narrow range between about  $7\text{--}30\%$  (Reid and Laronne, 1995;

Almedeij and Diplas, 2005). In contrast, the efficiency of sediment transport by steady base flow is about 0.04 times the flash flood efficiency and is typical for perennial streams with steady flow ( $0.00001\text{--}2\%$ ). A long-term time average of the remobilization and transport efficiencies for both transport processes for the period of the study would give a much lower efficiency ( $\sim 0.02\%$ , Fig. 6) than the average remobilization and transport efficiency for individual flash floods ( $0.18\%$ ). In the volcanic terrain the base flow ( $\sim 0.001 \text{ m}^3 \text{ s}^{-1}$ ; Table 1) was usually of insufficient magnitude to fill the alluvial bed, was subsurface flow, and could not transport sediment (Fig. 6). However, remobilization and transport efficiencies for individual flash floods ( $0.046\text{--}0.20\%$ ) were similar to those in the granitic terrain, but a similar long-term time average for the period of the study would be about an order of magnitude less ( $\sim 0.002\%$ ) than the granitic terrain. Thus, it might appear that the long-term erosion response is an order of magnitude greater in the granitic terrain than in the volcanic terrain, but the difference is really a function of the mean annual discharge and not the geology. However, comparing efficiencies associated with the sediment transport process (flash floods) shared by both terrains indicates that there is no difference in remobilization and transport efficiency.

#### 5.3.2. Hillslope

Sediment fluxes and efficiencies measured from bounded and unbounded plots are difficult to compare and the problem is exacerbated by different rainfall intensities in each terrain. Moreover, several hillslope transport processes can deliver sediment to the hillslope traps such as rainsplash, overland flow, rill, and rain-flow transport (Moss and Green, 1983; Abrahams et al., 1998; Gabet and Dunne, 2003). The bounded plots in the granitic terrain appear limited to sediment mobilized by rainsplash, overland flow, and rain-flow but these plots had sufficient lengths ( $\sim 5 \text{ m}$ ) for rills to develop. Rills have been shown to develop on laboratory plots (slope  $3.9^\circ$ ) within slope lengths of  $2.38\text{--}7.18 \text{ m}$  after 200 min of constant artificial rainfall ( $26 \text{ mm h}^{-1}$ ) (Bryan and Poesen, 1989). On steeper slopes rills may develop over shorter distances so that rill transport is possible within the bounded plots. Much depends on the rainfall intensity associated with each rainstorm. Rainfall intensity determines the contributing area or contributing distance to the traps, the runoff discharge, and the associated shear stress (Gilley et al., 1993) required to erode sediment along this distance. Sediment is not necessarily delivered by rill transport during every rainstorm, and during some rainstorms, it is possible that no sediment is transported by rills in either terrain. Each

rainstorm is different and produces a different proportion of the transport processes. Thus, we assumed the efficiencies from bounded and unbounded plots were comparable, when averaged over several rainstorms, because all transport processes were represented.

The previous discussion assumed equal sediment availability for the different geologic terrains. There may have been an important difference in the sediment availability because of the different start times for the hillslope measurements in the two terrains. In the granitic terrain, measurements were started after the first and largest rainstorm ( $I_{30} \sim 90 \text{ mm h}^{-1}$ ). This rainstorm created rills and easily removed a substantial portion of the fine component of the colluvium (10% silt and clay, 33% sand, and 57% gravel) stored on the hillslope leaving the gravel component to armor the hillslope. Widespread erosion of the available colluvium from the burned hillslopes was confirmed by aerial photographs and ground observations that indicated that a  $\sim 5 \text{ mm}$ -layer of ash and soil had been removed (Moody and Martin, 2001b). In contrast, measurements in the volcanic terrain were started before the largest rainstorm, the hillslope had no rills, and the hillslope was not armored. Most rainstorms in the volcanic terrain had relatively low rainfall intensity compared to the first storm in the granitic terrain (Fig. 4), and by themselves were unable to erode all of the available colluvium stored on the hillslope even though the colluvium (24% silt and clay, 60% sand, and 16% gravel) was finer than that in the granitic terrain. In the granitic terrain, the decrease in sediment availability was sudden leaving coarser colluvium that was more difficult to erode, while in the volcanic terrain the decrease was probably a slow, storm by storm decrease during the first summer after the wildfire. Thus, the average values of the remobilization and transport efficiencies partly reflect these differences in soil texture and temporal differences in sediment availability and may explain why the remobilization and transport efficiencies were greater in the volcanic terrain than in the granitic terrain.

We suspect that the initial detachment efficiency for the hillslope in the volcanic terrain was an underestimate because the first rainstorm (9 July 2000) had a lower rainfall intensity ( $I_{30} = 7.2 \text{ mm h}^{-1}$ ) than the next two storms on 16 and 18 July 2000 ( $I_{30} = 29 \text{ mm h}^{-1}$  for both). Unfortunately, the traps were overwhelmed with sediment and water overflowed the collecting containers during these two rainstorms. As a result, we were unable to calculate reliable initial detachment efficiencies for the storms. All efficiencies were  $>10\%$  for most traps possibly because of undetected overflow from the collecting containers. Again, this illustrates that had

the sequence of rainstorms following the wildfires been different, then these average efficiencies might have been quite different.

#### 5.4. Erodibility efficiencies in modeling

Erosion models must incorporate the dependence of the erodibility efficiencies on sediment availability. A simple empirical erosion model to predict transport rates from hillslopes was developed by Wilson (1999) based on runoff. The transport rate,  $W_h$ , from controlled rainfall simulation experiments with different intensities ( $36\text{--}162 \text{ mm h}^{-1}$ ) was related to the runoff or stream power. The best fit was a power law that can be written in a general form as

$$W_h = a(\omega_h - \omega_{hc})^p \quad (9)$$

where the critical stream power,  $\omega_{hc} = 0 \text{ J m}^{-2} \text{ s}^{-1}$ , the coefficient  $a = 0.18$ , and the exponent  $p = 1.9$  (Fig. 7). Our results for the granitic and volcanic terrains fit a linear relation ( $p = 1$ ;  $R^2 = 0.83$  and  $0.64$ , respectively) better than a power law relation ( $R^2 = 0.70$  and  $0.25$ , respectively). However, these linear relations, with  $\omega_{hc} = 0 \text{ J m}^{-2} \text{ s}^{-1}$  are biased and predict the large magnitude better than small magnitude sediment transport. The linear relation with  $\omega_{hc} \neq 0$  for the granitic terrain ( $\omega_{hc} = -0.011 \text{ J m}^{-2} \text{ s}^{-1}$ ;  $R^2 = 0.88$ ;  $p$  value  $< 0.001$ ) is slightly better than the relation using  $\omega_{hc} = 0$  and the negative value for the critical stream power may reflect the uncertainty or a small transport rate when the rainfall or stream power is zero (see dry ravel discussion below). The same is true for the volcanic terrain

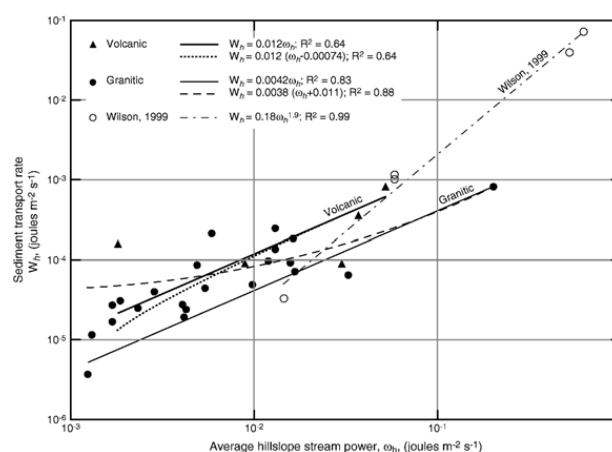


Fig. 7. Correlation of hillslope remobilization and sediment transport efficiencies with hillslope stream power. The short-dashed line is the relation determined by Wilson (1999) for artificial rain on burned plots in Tasmania. The solid lines are when the critical stream power is zero and the long-dashed lines when the critical stream power is not assumed to be zero.

where critical stream power  $\omega_{hc}=0.00074\approx 0 \text{ J m}^{-2} \text{ s}^{-1}$  ( $R^2=0.64$ ,  $p$  value=0.10). The values of the constant  $a$  (0.38% for granitic and 1.2% for volcanic terrain) are the least squares estimates of the remobilization and transport efficiencies and are about half the arithmetic averages of 0.65 and 2.4 (Table 3, Fig. 5), but have the about the same relative magnitudes. Fitting a linear relation ( $p=1$ ) to the data published by Wilson (1999) gives a value of the critical stream power ( $\omega_{hc}=0.043 \text{ J m}^{-2} \text{ s}^{-1}$ ), which is realistic for hillslopes (Elliot et al., 1989), and a remobilization and transport efficiency of 11%, which is larger than the remobilization and transport efficiencies for the granitic and volcanic terrains. This greater efficiency also may reflect the difference in sediment availability because Wilson (1999) noted that the fire destroyed a biotic surface crust protecting a loamy sand colluvium. This colluvium was probably more easily eroded than the granitic and volcanic soils in this paper.

Some of the variability of hillslope efficiencies may be a result of additional sediment transport processes like dry ravel. Dry ravel transport is an important process in some areas like southern California during the dry season (Krammes and Osborn, 1969). It has been measured in burned areas in granitic terrain in Colorado during dry periods between convective rainstorms in the summer and accounts for about 60% of the overland transport of sediment into hillslope traps (unpublished data). The negative value of  $\omega_{hc}$  for the granitic terrain could represent the contribution by dry ravel to the sediment transport rate when the rainfall and thus the stream power,  $\omega_h$ , was zero. Thus, in addition to erodibility efficiencies, models may need to incorporate other transport processes, sediment availability, and rainfall characteristics in order to accurately predict post-fire erosion.

## 6. Summary and conclusions

This study compared the erosional response after a wildfire in granitic and volcanic terrain. The erosion response was measured as the erodibility efficiency, which is the percentage of the total available stream power expended to detach, remobilize, or transport a mass of sediment. The efficiency permits the comparison of the erosion and deposition from a flood in one terrain that differs in magnitude from a flood in the second terrain. Erodibility efficiencies were estimated for the initial detachment efficiency of colluvium on the hillslope or sediment in the channels during the first rainstorm and flood after the fire and for the remobilization and transport efficiency of successive rainstorms and floods.

Contrary to expectations, the erosion response did not vary significantly between the two geologic terrains.

The initial detachment efficiencies for the main channel and a tributary channel in the granitic terrain were  $10\pm 9\%$  and  $5+4\%$  and in the volcanic terrain they were  $5\pm 5\%$  and  $1\pm 1\%$ . These initial detachment efficiencies are not unusually high for ephemeral channels and they may indicate that short timescale erosion processes, such as headcutting and bank failures, are more efficient than detachment by shear stress on the channel banks and bed—a processes typical of perennial streams (efficiencies  $\sim 0.00001$  to 1%). No initial detachment efficiency could be measured for the hillslopes in the granitic terrain because hillslope measurements were started after the first major rainstorm. The initial detachment efficiency in the volcanic terrain was  $1.3\pm 0.41\%$ .

The mass of eroded, transported, and deposited sediment depended on the sequence of rainstorms and floods. Remobilized and transported of sediment was primarily by episodic flash floods in both terrains with intervening periods of remobilization and transport by base flow in the granitic terrain. The average remobilization and transport efficiencies associated with flash floods in the channels also were similar in the granitic terrain ( $0.18\pm 0.57\%$ ) and in the volcanic terrain ( $0.11\pm 0.41\%$ ). The remobilization and transport efficiency on hillslopes was greater in the volcanic terrain (2.4%) than in the granitic terrain (0.65%). The lower efficiency in the granitic terrain probably reflects the reduced sediment availability as a result of the removal of fine colluvium by a large rainstorm ( $I_{30}\sim 90 \text{ mm h}^{-1}$ ) about 2 months after the wildfire, and the subsequent armoring of the hillslope surface before erosion measurements began. The remobilization and transport efficiency in the volcanic terrain was probably increased because available colluvium remained on the hillslope after the runoff from the first storm ( $I_{30}=7.2 \text{ mm h}^{-1}$ ). The hillslope sediment transport rates in volcanic and granitic terrains can be predicted by linear functions of hillslope stream power and the critical stream power.

## Acknowledgments

Field work in two geologic terrains cannot be done by three people. The ground surveys of the main channels and tributary channels were done with the help of Greg Alexander, Tanya Ariowitsch, Dave Kinner, Bob Meade, and Lisa Pine in the granitic terrain; and Erica Bigio, John Gartner, Neil Gray, Dave Kinner, Dave Mixon, and Brian Ragan in the volcanic terrain. Collecting and processing of the photogrammetric data was done by Dave Mixon, Eric White, and Dave Wolf. The installation and data collection from the hillslope traps were done with the help of Ellen Axtmann, Brent



Barkett, Mark Richards, and Lisa Pine in granitic terrain; and Erica Bigio, Jonathan Godt, and Edward Mine in the volcanic terrain. All made a conscientious effort to obtain data immediately after major convective rainstorms even if it meant being caught in another rainstorm. Clayton Jordan, Sandra Ryan-Burkett, and several anonymous reviewers made substantial suggestions that improved the paper.

## References

- Abrahams, A.D., Li, G., Krishnan, C., Atkinson, J.F., 1998. Predicting sediment transport by interrill overland flow on rough surfaces. *Earth Surface Processes and Landforms* 23, 1087–1099.
- Allison, R.J., Bristow, G.E., 1999. The effects of fire on rock weathering: some further considerations of laboratory experimental simulation. *Earth Surface Processes and Landforms* 24 (8), 707–713.
- Almedej, J., Diplas, P., 2005. Bed load sediment transport in ephemeral and perennial gravel bed streams. *EOS, Transactions, AGU* 86 (44), 429–434.
- Anderson, H.W., 1949. Flood frequencies and sedimentation from forest watersheds. *Transactions, AGU* 30 (4), 567–586.
- Bagnold, R.A., 1973. The nature of saltation and of 'bed-load' transport in water. *Proceedings of the Royal Society London A* 332, 473–504.
- Balice, R.G., Miller, J.D., Oswald, B.P., Edminster, C., Yool, S.R., 2000. Forest Surveys and Wildfire Assessment in the Los Alamos Region: 1998–1999. LA-13714-MS. Los Alamos National Laboratory, Los Alamos, NM. 86 pp.
- Benavides-Solorio, J.D., MacDonald, L.H., 2005. Measurement and prediction of post-fire erosion at the hillslope scale, Colorado front range. *International Journal of Wildland Fire* 14, 457–474.
- Bennett, S.J., Casali, J., 2001. Effect of initial step height on headcut development in upland concentrated flows. *Water Resources Research* 37 (5), 1475–1484.
- Blong, R.J., Riley, S.J., Crozier, P.J., 1982. Sediment yield from runoff plots following bushfire near Narrabeen Lagoon, NSW. *Search* 13 (1–2), 36–38.
- Booker, F.A., 1998. Landscape and management response to wildfires in California. Unpublished M.S. Thesis, Univ. of Calif., Berkeley, CA, 436 pp.
- Booker, F.A., Dietrich, W.E., Collins, L.M., 1995. The Oakland Hills fire of October 20, 1991: an evaluation of post-fire response. In: Keeley, J.E., Scott, T. (Eds.), *Brushfires in California Wildlands: Ecology and Resource Management*. International Association of Wildland Fire, Fairfield, WA, pp. 163–170.
- Brown, J.A.H., 1972. Hydrologic effects of a bushfire in a catchment in south-eastern New South Wales. *Journal of Hydrology* 15, 77–96.
- Bryan, R.B., Poesen, J., 1989. Laboratory experiments on the influence of slope length on runoff, percolation and rill development. *Earth Surface Processes and Landforms* 14, 211–231.
- Cannon, S.H., Kirkham, R.M., Parise, M., 2001a. Wildfire-related debris-flow initiation processes, Storm King Mountain, Colorado. *Geomorphology* 39, 171–188.
- Cannon, S.H., Bigio, E.R., Mine, E., 2001b. A process for fire-related debris flow initiation, Cerro Grande fire, New Mexico. *Hydrological Procedure* 15, 3011–3023.
- Cannon, S.H., Gartner, J.E., Parrett, C., Parise, M., 2003. Wildfire-related debris-flow generation through episodic progressive sediment-bulking processes, western USA. In: Rickenmann, D., Chen, C.L. (Eds.), *Debris-Flow Hazards Mitigation: Mechanics, Prediction, and Assessment*, Proceedings of the Third International Conference on Debris-flow Hazards Mitigation, Millpress, Rotterdam, pp. 71–82.
- Daniel, H.A., Elwell, H.M., Cox, M.B., 1943. Investigations in erosion control and reclamation of eroded land at the red plains conservation experiment station, Guthrie, Okla., 1930–40. Soil Conservation Service. Tech. Bull., vol. 837. USDA, Washington, DC. 93 pp.
- Darby, S.E., Alabayan, A.M., Vande Wiel, M.J., 2002. Numerical simulation of bank erosion and channel migration in meandering rivers. *Water Resources Research* 38 (9), 1163.
- DeBano, L.F., Conrad, C.E., 1976. The effect of fire on nutrients in a chaparral ecosystem. *Ecology* 59 (3), 489–497.
- DeBano, L.F., Dunn, P.H., Conrad, C.E., 1977. Fire's effects on physical and chemical properties of chaparral soils. Forest Service General Technical Report WO-3. USDA, Washington, DC, pp. 65–74.
- Doehring, D.O., 1968. The effect of fire on geomorphic processes in the San Gabriel Mountains, California. *Contributions to Geology* 7 (1), 43–65.
- Elliot, W.J., Liebenow, A.M., Laflen, J.M., Kohl, K.D., 1989. A compendium of soil erodibility data from WEPP cropland soil field erodibility experiments 1987 and 1988. NSERL report vol. 3, Ohio State Univ. and USDA Agric. Res. Ser., Columbus, OH, 316 pp.
- Florsheim, J.L., Keller, E.A., Best, D.W., 1991. Fluvial sediment transport in response to moderate storm flows following chaparral wildfire, Ventura County, southern California. *GSA Bull.* 103, 504–511.
- Gabet, E.J., Dunne, T., 2003. Sediment detachment by rain power. *Water Resources Research* 39 (1) (12 pp.).
- Gerits, J.J.P., De Lime, J.L.M.P., van de Broek, T.M.W., 1990. Overland flow and erosion. In: Anderson, M.G., Burt, T.P. (Eds.), *Process Studies in Hillslope Hydrology*. John Wiley, Hoboken, NJ, pp. 173–191.
- Gerlach, T., 1967. Hillslope troughs for measuring sediment movement. *Revue de Geomorphologie Dynamique* 17 (4), 173–174.
- Germanoski, D., Miller, J.R., Latham, D., 2002. The importance of event sequencing on the geomorphic impact of wildfire in the central Great Basin. *GSA Abstracts with Program* 34 (6), 319.
- Gilley, J.E., Elliot, W.J., Laflen, J.M., Simanton, J.R., 1993. Critical shear stress and critical flow rates for initiation rilling. *Journal of Hydrology* 142, 251–271.
- Giovannini, G., Lucchesi, S., Giachetti, M., 1988. Effects of heating on some physical and chemical parameters related to soil aggregation and erodibility. *Soil Science* 146, 255–261.
- Grant, G.E., 1997. Critical flow constrains flow hydraulics in mobile-bed streams: a new hypothesis. *Water Resources Research* 33 (2), 349–358.
- Griggs, R.L., Hem, J.D., 1964. Geology and ground-water resources of the Los Alamos area, New Mexico. Geological Survey Water-Supply Paper, vol. 1753. U.S. Government, Washington, DC, 107 pp.
- Jarrett, R.D., 1987. Errors in slope–area computations of peak discharges in mountain streams. *Journal of Hydrology* 96, 53–67.
- Kempton, K.A., Kelley, S., 2002. Geology of the Guaje Mountain 7.5-min. Quadrangle, Los Alamos and Sandoval Counties, New Mexico. Open-file Geologic Map OF-GM 55, scale 1:24,000, New Mexico Bureau of Geology and Mineral Resources, Washington, DC.
- Krammes, J.S., Osborn, J., 1969. Water-repellent soils and wetting agents as factors influencing erosion. In: DeBano, L.F., Letey, J. (Eds.), *Proc. of the Symp. on Water-Repellent Soils*. May 6–10, 1968. Univ. Calif., Riverside, pp. 177–187.



- Laird, J.R., Harvey, M.D., 1986. Complex-response of a chaparral drainage basin to fire. *Proc., Inter. Assoc. of Hydro. Sci. Conf.*, August 4–18, Hadley, R.F. (Ed.), Albuquerque, NM, IAHS Pub. 159, Drainage Basin Sediment Delivery, pp.165–183.
- Lavine, A., Kuyumjian, G.A., Reneau, S.L., Katzman, D., Malmon, D.V., 2006. A five-year record of sedimentation in the Los Alamos reservoir, New Mexico, following the Cerro Grande Fire. Joint 8th Federal Interagency Sedimentation Conference and 3rd Federal Interagency Hydrologic Modeling Conference. LA-UR-05\_7526\_paper.pdf, 8 pp.
- Martin, D.A., Moody, J.A., 2001. The flux and particle size distribution of sediment collected in hillslope traps after a Colorado Wildfire. *Proc. of the 7th Fed. Inter. Sediment. Conf.*, March 25–29, Reno, NV, pp. III-40–III-47.
- Megahan, W.F., Moliter, D.C., 1975. Erosional effects of wildfire and logging in Idaho. *Watershed Manage. Symp.*, August 11–13, Logan, Utah, ASCE Irrigation and Drainage Div., pp. 423–444.
- Miller, J.F., Frederick, R.H., Tracey, R.J., 1973. *Precipitation-frequency Atlas of the Western United States*, Colorado. NOAA Atlas 2, vol. III. Nat. Weather Ser., Washington, DC.
- Moody, J.A., 2001. Sediment transport regimes after a wildfire in steep mountainous terrain. *Proc. of the 7th Federal International Sediment. Conf.*, March 25–29, Reno, NV, pp. X-41–X-48.
- Moody, J.A., Martin, D.A., 2001a. Hydrologic and Sedimentologic Response of Two Burned Watersheds in Colorado. *Water Resources Invest. Rep.* 01-4122. U.S. Geological Survey, Denver, CO. 142 pp.
- Moody, J.A., Martin, D.A., 2001b. Initial hydrologic and geomorphic response following a wildfire in the Colorado Front Range. *Earth Surface Processes and Landforms* 26, 1049–1070.
- Moody, J.A., Smith, J.D., Ragan, B.W., 2005. Critical shear stress for erosion of cohesive soils subjected to temperatures typical of wildfires. *Journal of Geophysical Research* 110 (F01004), 1–13. doi:10.1029/2004JF000141.
- Moody, J.A., Martin, D.A., Haire, S.L., Kinner, D.A., in press. Linking runoff response to burn severity after a wildfire. *Hydrological Processes*.
- Moore, R., 1992. *Soil Survey of Pike National Forest, Eastern Part, Colorado, Parts of Douglas, El Paso, Jefferson, and Teller Counties*. U.S. Department of Agriculture, Forest Service and Soil Conservation Service, Washington, DC. 106 pp.
- Moss, A.J., Green, P., 1983. Movement of solids in air and water by raindrop impact, effects of drop-size and water-depth variations. *Australian Journal Soil Research* 21, 257–269.
- National Wildfire Coordinating Group, 1994. *Glossary of Wildland Fire Terms*. Publication PMS 205/NFES 1832. National Interagency Fire Center, Boise, Idaho, pp. II-1–II-27.
- Rantz, S.E., et al., 1982. *Measurement and Computation of Streamflow, Volume 1. Measurement of Stage and Discharge*. Water-Supply Paper, vol. 2175. U.S. Geological Survey, Washington, DC. 284 pp.
- Reid, I., Laronne, J.B., 1995. Bed load sediment transport in an ephemeral stream and a comparison with seasonal and perennial counterparts. *Water Resources Research* 31 (3), 773–781.
- Renard, K.G., Foster, G.R., Weesies, G.A., McCool, D.K., Yoder, D.C., 1997. Predicting soil erosion by water: a guide to conservation planning with the revised universal soil loss equation (RUSLE). U.S. Department of Agriculture Handbook, vol. 703. U.S. Government, Washington, DC, 404 pp.
- Reneau, S.L., Kuyumjian, G.A., Malmon, D.V., Tardiff, M.F., 2003. Precipitation-frequency relations on the Pajarito Plateau and in the eastern Jemez Mountains, New Mexico, and examples of extreme or flood-producing Storms. Los Alamos National Laboratory Report, LA-UR-03-6484. Los Alamos National Laboratory, Los Alamos, NM, 80 pp.
- Rich, L.R., 1962. Erosion and sediment movement following a wildfire in a Ponderosa Pine forest of central Arizona. Forest Service, Rocky Mount. Forest and Range Experiment Station. Research Notes, vol. 76. USDA, Fort Collins, CO. 12 pp.
- Robichaud, P.R., McCool, D.K., Pannkuk, C.D., Brown, R.E., Mutch, P.W., 2001. Trap efficiency of silt fences used in hillslope erosion studies. In: AscoughII II, J.C., Flanagan, D.C. (Eds.), *Proceedings of the International Symposium, Soil Erosion Research for the 21st Century*. American Society of Agricultural Engineers, St. Joseph, Michigan, pp. 541–543.
- Rowe, P.B., Countryman, C.M., Storey, H.C., 1954. Hydrologic analysis used to determine effects of fire on peak discharge and erosion rates in southern California. USDA Calif. Forest and range experiment station and University of California, Berkeley, CA, 49 pp.
- Ryan, K.C., Noste, N., 1985. Evaluating prescribed fires. In: Symposium and workshop on wilderness fire, Lotan, J.E., Kilgore, B.M., Fischer, W.C., Mutch, R.W. (Technical Coordinators). Missoula, MT, pp. 230–238.
- Santi, P.M., deWolfe, V.G., Higgins, J.D., Cannon, S.H., Gartner, J.E., in press. Sources of debris-flow material from burned areas. *Geomorphology* (Available online 10 May 2007).
- Scott, D.F., Versfeld, D.B., Lesch, W., 1998. Erosion and sediment yield in relation to afforestation and fire in the mountains of the Western Cape Province, South Africa. *So. African Geogr. Journal* 80 (1), 52–59.
- Shaull, D.A., Alexander, M.R., Reynolds, R.P., McLean, C.T., Romero, R.P., 2000. Surface water data at Los Alamos National Laboratory: 1999 Water Year. LA-13706-PR, p. 72.
- Simon, A., Collison, A.J.C., 2001. Pore-water pressure effects on the detachment of cohesive streambeds: seepage forces and matric suction. *Earth Surface Processes and Landforms* 26, 1421–1442.
- Simon, A., Curini, A., Darby, S.E., Langendoen, E.J., 1999. Stream-bank mechanics and the role of bank and near-bank processes in incised channels. In: Darby, S.E., Simon, A. (Eds.), *Incised River Channels*. John Wiley & Sons, Ltd., New York, NY, pp. 123–152. Chapter 6.
- Smith, J.D., 2004. The role of riparian shrubs in preventing floodplain unraveling along the Clark Fork of the Columbia River in the Deer Lodge Valley, Montana. *Riparian Vegetation and Fluvial Geomorphology*. Water Science and Application, vol. 8. AGU, Washington, DC, pp. 71–85.
- White, W.D., Wells, S.G., 1984. Geomorphic effects of la mesa fire. In: Foxx, T.S. (Ed.), *La Mesa Fire Symposium*, Los Alamos, New Mexico, October 6 and 7, 1981. Los Alamos National Laboratory, Los Alamos, NM, pp. 73–90. LA-9236-NERP.
- Wiberg, P., Smith, J.D., 1987. Calculation of the critical shear stress for motion of uniform and heterogeneous sediments. *Water Resources Research* 23 (8), 1471–1480.
- Wilson, C.J., 1999. Effects of logging and fire on runoff and erosion on highly erodible granitic soils in Tasmania. *Water Resources Research* 35 (11), 3531–3546.
- Yang, C.T., 1972. Unit stream power and sediment transport. *Journal Hydraul. Div., ASCE*, HY10, 1805–1825.